Chapter 5: Optical & Electrical Characterization

As is well known the transparent conducting oxides (TCOs) have applications in the fields of electrical devices and displays [1–3]. For these applications, the TCOs should have two important properties i.e. good electrical conduction and transmittance in visible region. Indium tin oxide (ITO) is the popular choice as TCO material due to its high electrical conductivity and greater optical transmittance. However due to its scaracity, high product cost, and environmental pollution problems associated with of ITO, the workers are trying to look for alternative of ITO. Among other TCO materials, ZnO and SnO_2 are good choices [4, 5]. ZnO is a promising alternative to ITO, because it is non-toxic, inexpensive, highly abundant, especially stable in hydrogen plasma, and undergoes crystallization at low decomposition temperature [6]. There are many characteristics of ZnO that makes it suitable for efficient utilization in various novel devices. ZnO is an n-type semiconductor with a wide band gap of 3.37 eV with large exciton binding energy (60 meV) [7].

Recent research shows that ZnO nanomaterials are promising piezoelectric nano generators. This fact has trigs a wide range of subsequent research in searching for new synthetic methods to synthesize ZnO nanomaterials [2]. Among the various ZnO nanostructures, ZnO nanoparticles are the most frequently studied [3], due to their relevance in fundamental study and also because their applications in the field of solar energy conversion, photo catalysis, light-emitting materials [4], transparent UV protection films and chemical sensors [5]. Until now, a variety of techniques have been employed for the synthesis of ZnO nanoparticles, such as metal organic chemical vapour deposition (MOCVD), spray pyrolysis, ion beam assisted deposition, laser-ablation, sputter deposition, template assisted growth and chemical vapor deposition [6–13]. Although the ZnO nanoparticles fabricated using the above methods have a high-purity and high-crystalline structure, but the growth temperature is too high to make them compatible with low-temperature endurance substrates such as glass. Therefore, we need to look for a low-temperature, large-scale, and simple synthetic process for the synthesis of ZnO nanoparticles, which can subsequently be used for nanoscale devices. In this chapter, we present the successful synthesis of ZnO nanoparticles on glass substrate using a simple physical vapor condensation method at a temperature as low as 400^{O}C. The optical and electrical properties of this film containing ZnO nanoparticles were also studied in the wavelength of 300-900 nm and temperature range of 450-300K respectively.

5.1 Experimental

Thin film of ZnO is deposited by physical vapour condensation method. In this method, the starting material is Zn powder (99.999 % pure), which is heated at a temperature of 400^{O}C in presence of oxygen and argon gases in the chamber. Initially a small quantity of Zn powder was kept in a molybdenum boat and the chamber was evacuated to a vacuum of the order of 10^{-6} Torr. After attaining this vacuum, the gases (oxygen and argon) are purged in to the chamber. The pressure of these gases is kept fixed at 16 mbar and 4 mbar respectively. The substrate is cooled with liquid nitrogen and this evaporated material is deposited on glass substrate pasted on

ISBN: 978-81-942709-0-4
Thesis DOI: 10.21467/thesis.78

the LN_2 cooled substrate. The nanoparticles of ZnO are deposited on the glass substrate and also collected in the powder form by scratching from the substrate. Powder X-ray diffraction (XRD) is performed using a Philips X-ray diffractometer with Cu Kα (l ¼ 1:54178 Å) radiation. The morphology and the microstructure of these nanostructures are studied using a Joel field emission scanning electron microscope (FESEM 7500f) and transmission electron microscope (TEM) at 100 kV. UV–VIS absorption spectrum is recorded using a V-570 Jasco UV–Vis double-beam spectrophotometer. The scanning wavelength range is 300–900 nm. In this investigation, we have successfully grown the ZnO nanoparticles at low temperatures, keeping the gases (O2 and Ar) flow fixed at 6 mbar and 4 mbar respectively.

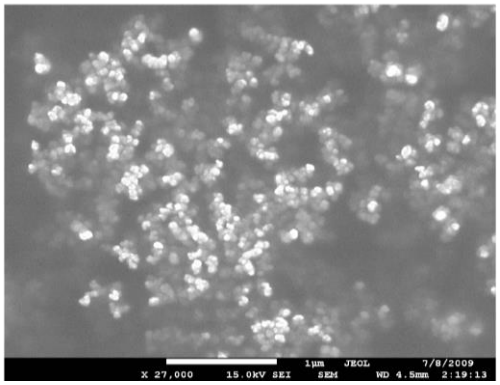

Figure 5.1:(a) *FESEM image of ZnO nanoparticles*

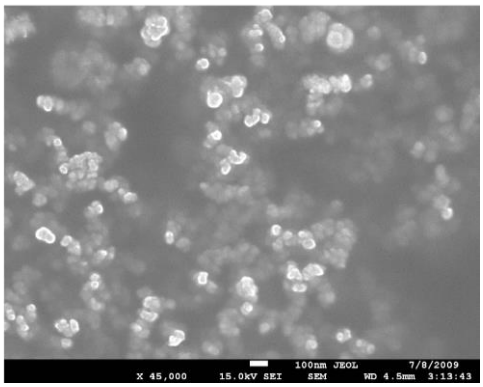

Figure 5.1: (b) *FESEM image of ZnO nanoparticles*

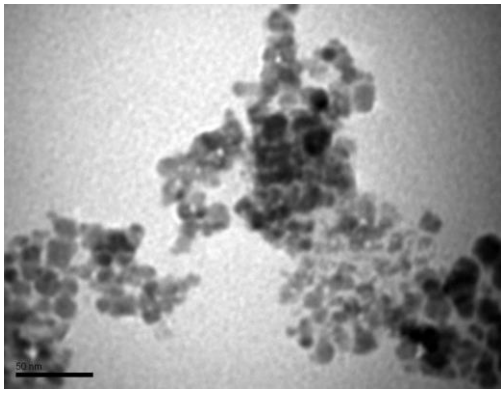

Figure 5.2: *(a) TEM image of ZnO nanoparticles*

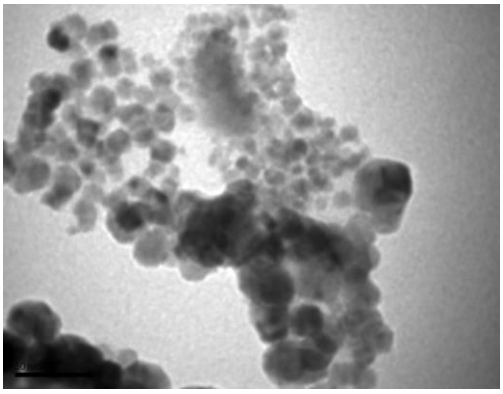

Figure 5.2: (b) *TEM image of ZnO nanoparticles*

5.2 Results and discussion

The field emission scanning electron microscope (FESEM) images of the thin film of ZnO are presented in Figures 5.1 (a) & (b). FESEM images reveal the typical morphologies of the grown ZnO nanoparticles. These nanoparticles look like clusters of two or more particles. The size of these nano clusters varies from 30-80 nm. It is observed from the TEM image (Figures 5.2 (a) & (b)) that the typical diameter of these nanoparticles obtained is in the range of 5 to 20 nm. The typical X-ray diffraction (XRD) pattern of these nanoparticles is

presented in Figure 5.3. The XRD spectrum shows that the deposition in the presence of oxygen leads to the formation of ZnO nanoparticles on the glass substrate. In the process used, the source material is heated at 400^{o}C in the presence of oxygen. During this oxidation process, the starting material (Zn) is converted into ZnO film with a polycrystalline structure. The peaks at 36.6^{o} and at 32^{o} are associated with ZnO (101) and ZnO (100) crystallographic plane.

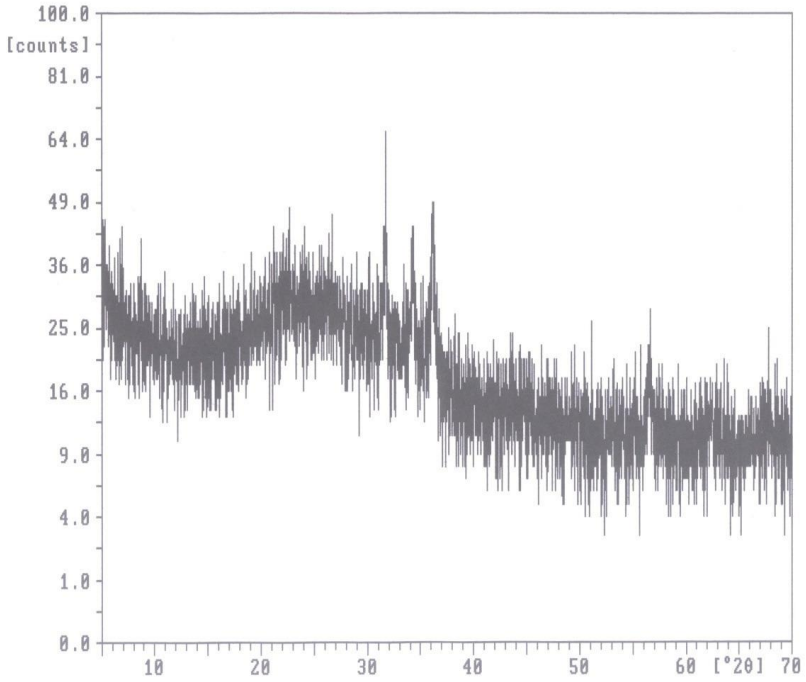

Figure 5.3: *XRD pattern of ZnO thin film*

The XRD spectrum very clearly demonstrates that the film deposited in oxygen atmosphere has a dominant (101) orientation. A peak associated with Zn is also observed at 57^{o}. These peaks match with JCPDS data (JCPDS 36-1451). We have employed a V-570 Jasco UV–Vis double-beam spectrophotometer for recording the optical absorption of the ZnO film. The scanning wavelength range is 300–900 nm. The absorption is measured in terms of optical density. Thin film of ZnO deposited glass substrate and reference (glass) is kept inside the appropriate film holder. The optical absorption is measured as a function of incidence wavelength.

The absorption coefficient (α) is calculated using the following relation;

$$\alpha = OD/t \qquad (5.1)$$

where OD is the optical density measured at a given film thickness (t).

Figure 5.4 shows the variation of the absorption coefficient (α) as a function of incident photon energy ($h\nu$) for ZnO film. The value of absorption coefficient increases exponentially with the increase in photon energy. In both crystalline and amorphous materials, the exponential dependence of absorption coefficient on energy may arise from the random fluctuations of internal fields associated with the structural disorder/intrinsic defects

such as zinc interstitials and oxygen vacancies [14] The dependence of optical absorption coefficient on photon energy may arise from electronic transitions between localized states.

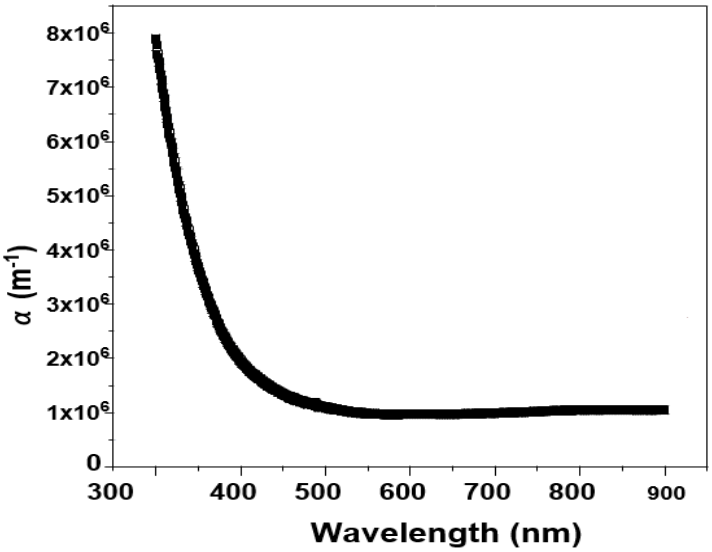

Figure 5.4: *Optical absorption (α) Vs wavelength of ZnO thin film in the wavelength range of (400-900 nm)*

The density of these states falls off exponentially with energy. This behavior is consistent with the theory of Tauc [14] The absorption coefficient near fundamental absorption edge is exponentially dependent on the incident photon energy and obeys the empirical Urbach relation,

where lnα varies as a function of hν. Urbach energy can be calculated by the following relation [15],

$$a = a_o \exp(h\nu - EI / E_U) \quad (5.2)$$

where E_I and α_o are constants and E_U is the Urbach energy which refers to the width of the exponential absorption edge. Figure 5.5 shows the variation of ln α vs. photon energy for the films. The E_U value was calculated from Urbach plots using the relationship

$$E_u = [d(\ln\alpha)/d(h\nu)]^{-1} \quad (5.3)$$

The value of Urbach energy (E_U) is also calculated using the slope of the plot ln α vs. photon energy and it is found to be 805.8 meV. This value of Urbach energy is comparable with that reported by other workers [19].

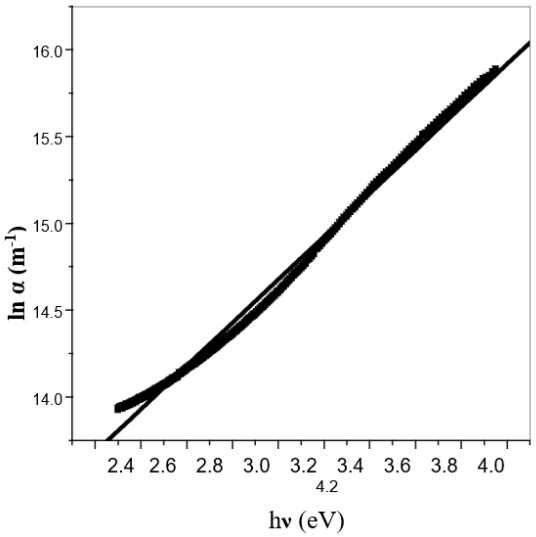

Figure 5.5: *ln α Vs hν plot for ZnO thin film*

In case of semiconductors, the fundamental absorption edge follows an exponential law. Above the exponential tail, the absorption coefficient has been reported [15] to obey the following equation:

$$(\alpha h\nu)^{1/n} = B(h\nu - Eg) \qquad (5.4)$$

where ν is the frequency of the incident beam (ω=2πν) , B is a constant, E_g is optical band gap, n is an exponent and it can have various values e.g. 1/2, 3/2, 2 and 3 depending on the nature of electronic transition responsible for the absorption. For allowed direct transition, n can have a value of either 1/2 or 3/2 and for forbidden indirect transition, n can have a value of either 2 or 3 [16]. Here, the direct and indirect transitions are optical transitions that occur in the crystalline semiconductors. It is well known that direct transition across the band gap is feasible between the valence and the conduction band edges in k space. In the transition process, the total energy and momentum of the electron–photon system must be conserved.

It is found that our experimental data recorded for ZnO film gives a best fit with n = 1/2 using equation (4). This suggests that the absorption in ZnO film is due to direct transition. Therefore, the experimental data is re-plotted as $(\alpha.h\nu)^2$ Vs photon energy (hν) for direct transition. Figure 5.6 presents the variation of $(\alpha.h\nu)^2$ with photon energy (hν) for ZnO film. The value of direct optical band gap (E_g) is calculated by measuring the intercept on the X-axis. The calculated value of E_g for the present ZnO sample is 3.54 eV. This value is comparable with the results of various workers for other ZnO nanostructures reported in the literature [17-18].

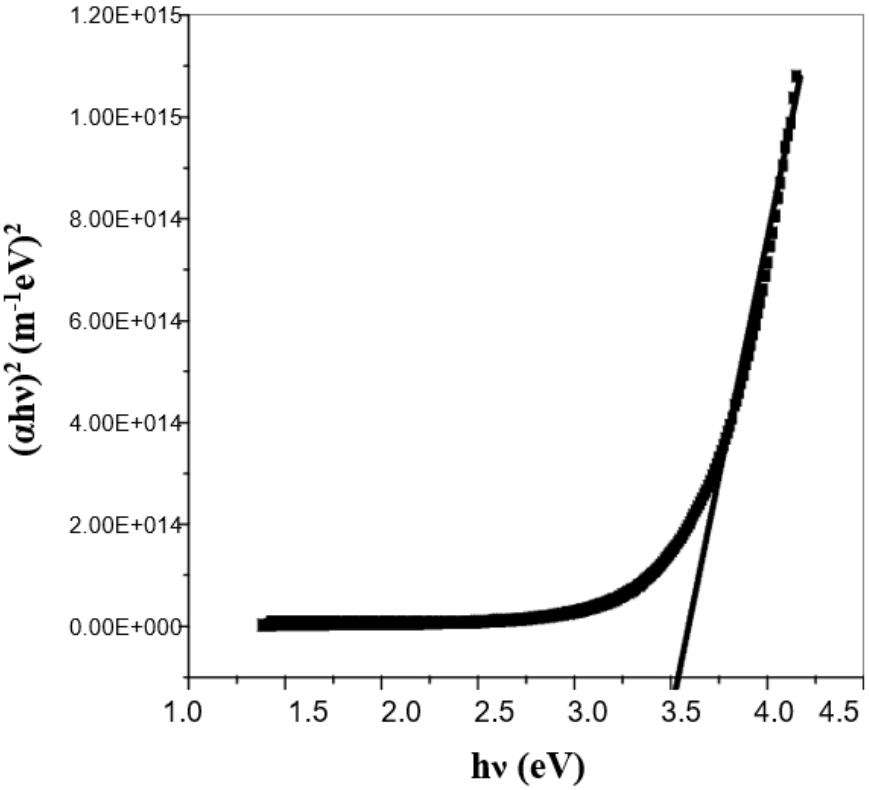

Figure 5.6: *$(\alpha h\nu)^{1/2}$ Vs hν for ZnO thin film in the wavelength range of (400-900 nm)*

Electrical conductivity in thin film of ZnO can proceed through a variety of mechanisms. Intrinsic defects in ZnO are notorious for their electrical activity, and along with extrinsic impurities, can give rise to impurity conduction phenomena and band conduction, near and above room temperature. In addition, the grain boundaries act as charge-carrier traps, leading to band bending and potential barriers all around the grains, thus affecting the electrical conductivity of this film [20]. This process may be taken into consideration for explaining the electrical conduction mechanism in the sample.

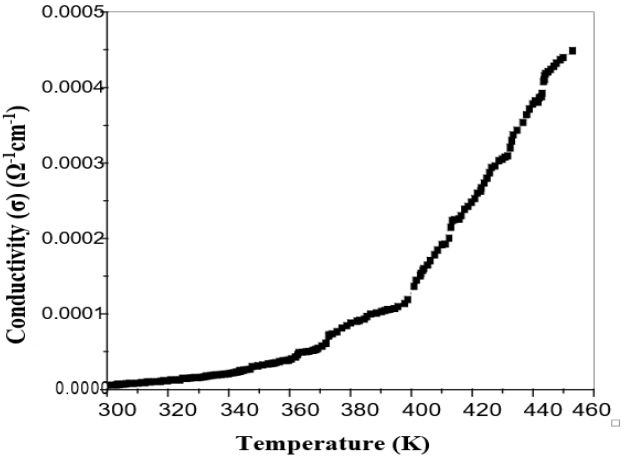

Figure 5.7: *Variation of conductivity (σ) Vs Temperature for ZnO thin film for the temperature range of (450-300K)*

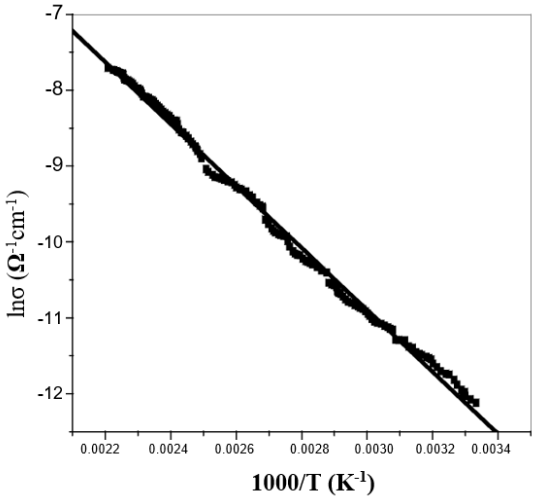

Figure 5.8: *ln σ Vs 1000/T for ZnO thin film for the temperature range of (450 - 300K)*

Temperature dependence of dc conductivity for the temperature range (450-300K) is presented in Figure 5.7. The dc conductivity varies exponentially with the temperature. For the present sample of ZnO thin film, the conductivity as a function of temperature shows Arrhenius behavior. The plot of lnσ Vs 1000/T for the temperature range of (450-300K) is presented in Figure 5.8. It is observed that the plot of lnσ Vs 1000/T is a straight line, which suggests that the conduction in this system is through thermally activated process. The conductivity, can therefore be expressed by the usual relation

$$\sigma = \sigma_0 \exp(-\Delta E/k_B T) \qquad (5.5)$$

where ΔE is the activation energy and k_B is Boltzmann constant. The value of E calculated using the slope of Figure 5.8, is found to be 0.35 eV. As mentioned before, the present sample is grown in oxygen environment. In such a situation, the carriers are likely to originate in intrinsic defects such as zinc interstitials and oxygen vacancies. These defects are generally recognized as the source of n-type conductivity commonly observed in ZnO nanostructures grown in oxygen rich environment, producing defect levels that lie below the conduction band [21]. Therefore, the present sample exhibits n-type semiconducting behavior originating from native defects, mainly of Zn interstitials or oxygen vacancies.

5.3 Conclusion

From the above studies, it is concluded that the thin film of ZnO contains nanoparticles with the diameter varying from 5-20nm. The XRD spectrum shows the peaks at 36.6° and at 32° which are close to the characteristic peak of ZnO. In case of optical properties, the absorption mechanism is due to direct transition and the value of the optical band gap is found to be 3.54 eV. It has been observed that the absorption coefficient increases exponentially with the increase in photon energy. The value of Urbach energy (E_U) is also calculated using the slope of the plot ln α vs. photon energy and is found to be 805.8 meV. Electrical conduction mechanism is successfully explained with thermally activated transport for the temperature range of 450-300K. For thermally activated process, the calculated value of activation energy is 0.35 eV. The present sample exhibits *n*-type semiconducting behavior originating from native defects, mainly of Zn interstitials or oxygen vacancies.

5.4 References

[1] C. Pacholski, A. Kornowski, H. Weller, Angew. Chem. Int. Ed. Engl. 43 (2004) 4774.

[2] Z.L.Wang, J. Song, Science 312 (2006) 242.

[3] R. Turgeman, S. Tirosh, A. Gedanken, Chem. Eur. J. 10 (2004) 1845.

[4] G.R. Gattorno, P.S. Jacinto, L.R. Va'zquez, J. Phys. Chem. B 107 (2003) 12597.

[5] E. Meulenkamp, J. Phys. Chem. B 102 (1998) 5566.

[6] K. Haga, F. Katahira, H.Watanabe, Thin Solid Films 343 (1999) 145.

[7] K. Ogata, T. Kawanishi, K. Maejimaz, K. Sakurai, S. Fujita, Jpn. J. Appl. Phys. 7A (2001) 240.

[8] S.A. Studenikin, N. Golego, M. Cocivera, J. Appl. Phys. 84 (1998) 2287.

[9] W. Li, D.S. Mao, Z.H. Zheng, X. Wang, X.H. Liu, S.C. Zhu, Q. Li, J.F. Xu, Surf. Coat. Technol. 346 (2000) 128.

[10] Y. Sun, G.M. Fuge, M.N.R. Ashfold, Chem. Phys. Lett. 396 (2004) 21.

[11] W. Chiou,W.Wu, J. Ting, Diam. Relat. Mater. 12 (2003) 1841.

[12] Y. Li, G.W. Meng, L.D. Zhang, Appl. Phys. Lett. 76 (2000) 2011.

[13] S.Y. Li, C.Y. Lee, T.Y. Tseng, J. Cryst. Growth 247 (2003) 357.

[14] J. Tauc, Amorphous and Liquid Semiconductors, Plenum Press, New York, 1974.

[15] F. Urbach, Phys. Rev. 92 (1953) 1324.

[16] A.A. Al-Ghamdi, Vacuum 80 (2006) 400.

[17] Dhananjay, J. Nagaraju, S.B. Krupanidhi, Materials Science and Engineering B 133 (2006) 70–76.

[17] L. M. Kukreja, S. Barik and P. Misra Journal of Crystal Growth 268 (3-4) (2004) 531-535.

[18] Fahrettin Yakuphanoglua, Yasemin Caglarb, Saliha Ilicanb, Mujdat Caglar, Physica B 394 (2007) 86–92

[19] Y. Natsume, H. Sakata, T. Hirayama, H. Yanagida, J. Appl. Phys. 72 (1992) 4203.

[20] S.J. Pearton, D.P. Norton, K. Ip, Y.W. Heo, J. Vac. Sci. Technol., B 22 (2004) 932.